Adaptive Neural Network Control of an Uncertain 2-DOF Helicopter With Unknown Backlash-Like Hysteresis and Output Constraints

Zhijia Zhao, *Member, IEEE*, Jian Zhang, Zhijie Liu, *Member, IEEE*, Chaoxu Mu, *Senior Member, IEEE*, and Keum-Shik Hong, *Fellow, IEEE*

***Abstract*— An adaptive neural network (NN) control is proposed for an unknown two-degree of freedom (2-DOF) helicopter system with unknown backlash-like hysteresis and output constraint in this study. A radial basis function NN is adopted to estimate the unknown dynamics model of the helicopter, adaptive variables are employed to eliminate the effect of unknown backlash-like hysteresis present in the system, and a barrier Lyapunov function is designed to deal with the output constraint. Through the Lyapunov stability analysis, the closed-loop system is proven to be semiglobally and uniformly bounded, and the asymptotic attitude adjustment and tracking of the desired set point and trajectory are achieved. Finally, numerical simulation and experiments on a Quanser's experimental platform verify that the control method is appropriate and effective.**

***Index Terms*— Adaptive neural network (NN) control, output constraint, two-degree of freedom (2-DOF) helicopter, unknown backlash-like hysteresis.**

I. Introduction

UNMANNED aerial vehicles (UAVs) have attracted widespread attention with the continuous development of science and technology [1]–[4]. Helicopters, as a typical UAV, have the advantages of flexible flight, strong adaptability, hovering flight, and so on and are widely used in air transportation, detection rescue, aviation mapping, and other fields [5], [6]. However, the helicopter system is a highly cross-coupled multi-input–multioutput (MIMO) nonlinear system involving complex dynamics, which makes the robust control design of the helicopter system more complicated [7]–[9]. Therefore, it is necessary to establish an effective control strategy to maintain the robustness and stability of helicopter systems.

Over the past decade, researchers have proposed a variety of control techniques for a stable control of helicopter systems [10]–[15]. For instance, in [11], a sliding mode control (SMC) based on a high-order disturbance observer was proposed and validated on a two-degree of freedom (2-DOF) helicopter. Chun *et al.* [12] proposed a new Q-learning algorithm to solve the unknown discrete-time linear quadratic regulation (LQR) adjustment problem and demonstrated the effectiveness of the approach on 2-DOF helicopter systems. In [13], for a 2-DOF helicopter system subjected to external interferences and uncertainties, the authors proposed an adaptive LQR algorithm. Furthermore, in [15], a flight controller was designed to track and control the model-based helicopter system. Note that, in the previous research, the nonlinear dynamics of the helicopter was linearized and the nonlinear term and uncertainties of the helicopter system were ignored, which may make the helicopter system unstable in practical applications. Therefore, it is necessary to incorporate the nonlinear dynamics of the helicopter system when designing a high-performance controller. For the helicopter's nonlinear dynamics, the researchers investigated a large number of control methods [16]–[18]. Raptis *et al.* [16] designed a backstepping control strategy to track the desired position and attitude of a 2-DOF helicopter. In [17], an SMC strategy with a generalized proportional integral observer was developed for 2-DOF helicopters influenced by extrinsic disturbances. Anis and Tarek [18] proposed a generalized robust predictive control and verified the reliability of the algorithm on a 2-DOF helicopter platform. However, the above research only considered that the nonlinear dynamics of the helicopter were accurately known and did not consider the case that some model parameters of the helicopter system are unknown and uncertain in the actual situation.

Manuscript received September 15, 2021; revised January 26, 2022; accepted March 25, 2022. This work was supported in part by the National Natural Science Foundation of China under Grant 61803109, Grant 61903196, and Grant 51905115; in part by the Science and Technology Planning Project of Guangzhou City under Grant 202102010398, Grant 202102010411, and Grant 202102010403; in part by the Scientific Research Projects of Guangzhou Education Bureau under Grant 202032793; in part by the Open Research Fund from the Guangdong Laboratory of Artificial Intelligence and Digital Economy (SZ) under Grant GML-KF-22-27; in part by the Guangzhou University Graduate Student Innovative Research Grant Program under Grant 2021GDJC-M30; in part by the Tianjin Natural Science Foundation under Grant 20JCYBJC00880; and in part by the Korea Institute of Energy Technology Evaluation and Planning through the Auspices of the Ministry of Trade, Industry and Energy, Republic of Korea, under Grant 20213030020160. *(Corresponding author: Zhijie Liu.)*

Zhijia Zhao and Jian Zhang are with the School of Mechanical and Electrical Engineering, Guangzhou University, Guangzhou 510006, China, and also with the Guangdong Laboratory of Artificial Intelligence and Digital Economy (SZ), Shenzhen 518060, China (e-mail: zhjzhaoscut@163.com; zhangjian041715@163.com).

Zhijie Liu is with the Institute of Artificial Intelligence and the State Key Laboratory of Advanced Metallurgy, University of Science and Technology Beijing, Beijing 100083, China (e-mail: liuzhijie2012@gmail.com).

Chaoxu Mu is with the School of Electrical and Information Engineering, Tianjin University, Tianjin 300072, China (e-mail: cxmu@tju.edu.cn).

Keum-Shik Hong is with the School of Mechanical Engineering, Pusan National University, Busan 46241, South Korea (e-mail: kshong@pusan.ac.kr).

Color versions of one or more figures in this article are available at https://doi.org/10.1109/TNNLS.2022.3163572.

Digital Object Identifier 10.1109/TNNLS.2022.3163572

In recent years, the research on the uncertainties of nonlinear systems has received extensive attention from researchers. Neural networks (NNs) have good approximation capabilities and are typically and commonly used tools to deal with system uncertainties [19]–[23]. For example, for 3-DOF helicopter systems with unknown dynamics model and subject to external perturbations, Yang and Zheng [24] proposed a backstepping control based on NN. In [25], for an unmanned helicopter system subjected to unknown internal and external disturbance, the authors proposed an adaptive NN active antidisturbance control strategy. In [26], for quadrotor UAVs with external disturbances and actuator failures, the authors proposed an NN fault-tolerant control. In [27], for a quadrotor UAV system with only position and attitude measurement, the authors proposed a novel output feedback NN control strategy. Nodland *et al.* [28] proposed a new high-performance NN optimal control for output feedback trajectory tracking of unmanned helicopter systems.

On the other hand, hysteresis is widely present in many practical electronic equipment actuator systems. The existence of hysteresis may degrade the performance of actuators, increase the error of the system or oscillation, and result in system instability [29]–[31]. Therefore, when designing system controllers, it has always been a research hotspot to decrease the effect of hysteresis. Moreover, the backlash-like hysteresis has good hysteresis nonlinear characteristics, which is conducive to the controller design [32], [33]. In recent years, many constructive control schemes have been proposed for nonlinear systems with unknown backlash-like hysteresis [34]–[40]. In [35], an adaptive NN control scheme was proposed for stochastic nonlinear systems with backlash-like hysteresis. In [36], considering the existence of state constraints and hysteresis in single-input–single-output nonlinear systems, the authors developed an adaptive control strategy in combination with backstepping control. In [38], for a type of flexible manipulator system with actuator failure, backlash-like hysteresis, and external environmental interference, a boundary adaptive fault-tolerant control was proposed. In [40], a Nussbaum gain technique was utilized to address the effect of unknown hysteresis in the system and an adaptive NN control technique was proposed. Although the above research on backlash-like hysteresis has made remarkable progress, there is no research on the 2-DOF helicopter nonlinear system with unknown backlash-like hysteresis.

Generally, there are various constraints in the actual control system, such as state constraints and output constraints [41]–[43]. If these constraints are ignored when designing the control, it may decrease the system's stability and even cause serious accidents [44]–[47]. Therefore, the researchers have proposed many effective control methods to address the system's constraints in recent years. For example, in [48], to solve the asymmetric full-state constraints in MIMO nonlinear systems, the authors designed an effective robust adaptive dynamic surface control. It is worth noting that, to resolve the output constraint in nonlinear systems, the use of a barrier Lyapunov function (BLF) is an effective method [49]. The BLF in [50] was first used to solve the output constraints of nonlinear systems. Zhao and Song [51] proposed a new robust adaptive control strategy to address the constraints in the conventional BLF or integral BLF control for a strict feedback nonlinear systems with full-state constraints depending on a virtual controller. Zhao and Chen [52] constructed a novel potential function to solve the asymmetric time-varying output constraint in MIMO nonlinear systems. Zhao *et al.* [53] proposed a new adaptive control strategy based on a generic potential function for solving asymmetric output constraints in pure feedback nonlinear systems. In the actual 2-DOF helicopter nonlinear system, the helicopter's movement is restricted by the environment, that is, the output of the helicopter is restricted. If the above limitations are not considered, the helicopter system may be unstable. Therefore, it is necessary to consider the issue of helicopter's output constraints, use a BLF to limit the output of the system to a fixed range, and at the same time guarantee that the system's tracking errors converge near zero.

Based on the analysis and summary of the above literature, we intend to establish an adaptive NN control for the 2-DOF helicopter nonlinear system with unknown backlash-like hysteresis and output constraints in this study. The main contributions are given as follows.

1) The backlash-like hysteresis is considered for the first time in a 2-DOF helicopter system, and adaptive variables with an adaptive NN control are developed to tackle the unknown hysteresis, eliminate the uncertainties, and improve the robustness of the system.
2) Using the BLF technology to constrain the output of the 2-DOF helicopter system, the system's tracking errors are ensured to converge near zero.
3) The control algorithm is tested on a Quanser's 2-DOF helicopter experimental platform, and the experimental results obtained verify the feasibility and effectiveness of the proposed control strategy.

The remaining chapters of this article are given as follows. In Section II, the helicopter system model, the backlash-like hysteresis, and some preliminary lemmas are introduced. Section III introduces the controller design. Section IV simulates and verifies the proposed controller. In Section V, we conduct an experimental verification and the results are given. Section VI gives a summary.

II. Problem Formulation and Preliminaries

A. Problem Formulation

Fig. 1 shows a 2-DOF helicopter model diagram [54]. It can be seen from the figure that the horizontally placed propeller will generate a torque around the Y-axis and get a pitch angle θ, and the vertically placed propeller will produce a torque around the Z-axis and get a yaw angle ϕ. In the 2-DOF helicopter system, the outputs are the pitch and yaw angles, and the input is the voltage in the dc motor that controls the pitch and yaw angles.

According to the Lagrangian mechanical modeling, the nonlinear dynamic equations of the system

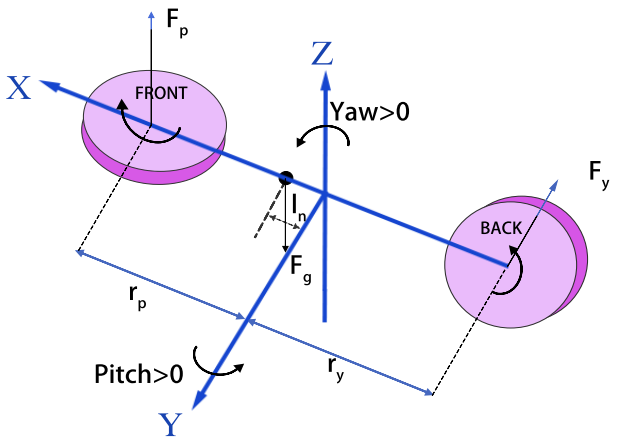

Fig. 1. 2-DOF helicopter model diagram.

are formulated as follows:

$$\begin{aligned}\left(J_p + M_a l_n^2\right)\ddot{\theta} &= K_{pp}V_p + K_{py}V_y - M_a g l_n \cos\theta \\ &\quad - D_p\dot{\theta} - M_a l_n \dot{\phi}^2 \sin\theta\cos\theta \qquad (1)\\ \left(J_y + M_a l_n^2\cos^2\theta\right)\ddot{\phi} &= K_{yp}V_p + K_{yy}V_y - D_y\dot{\phi} \\ &\quad + 2M_a l_n^2 \dot{\phi}\dot{\theta}\sin\theta\cos\theta \qquad (2)\end{aligned}$$

where θ and ϕ are the pitch and yaw angles, respectively, g represents the acceleration of gravity, D_p and D_y denote the viscous friction coefficients of the pitch and yaw axes, respectively, J_p and J_y are the rotational inertia around the pitch and yaw axes, respectively, l_n denotes the length of the helicopter, M_a indicates the weight of the helicopter, and K_{pp}, K_{py}, K_{yp}, and K_{yy} are the thrust torque constants generated by the helicopter system [54].

Define $x = [x_1, x_2]^T$, $x_1 = [\theta, \phi]^T$, and $x_2 = [\dot{\theta}, \dot{\phi}]^T$. Considering the backlash-like hysteresis and output constraints of the system, we convert the 2-DOF helicopter system into an MIMO system, which yields

$$\dot{x}_1 = x_2 \qquad (3)$$

$$\begin{aligned}\dot{x}_2 &= F(x) + \Delta F(x) \\ &\quad + (G(x) + \Delta G(x))\Phi(u) \qquad (4)\end{aligned}$$

$$y = x_1 \qquad (5)$$

where $u = [V_p, V_y]$ denotes the control input, $\Delta F(x)$ and $\Delta G(x)$ are system uncertainties, and $\Phi(u)$ represents the output of the backlash-like hysteresis. $F(x)$ and $G(x)$ are given as

$$F(x) = \begin{bmatrix} \dfrac{-M_a g l_n \cos(x_{11}) - D_p x_{21} - M_a l_n^2 x_{12}^2 \sin(x_{11})\cos(x_{11})}{J_p + M_a l_n^2} \\ \dfrac{-D_y x_{22} + 2M_a l_n^2 x_{22} x_{21}\sin(x_{11})\cos(x_{11})}{J_y + M_a l_n^2\cos^2(x_{11})} \end{bmatrix} \qquad (6)$$

$$G(x) = \begin{bmatrix} \dfrac{K_{pp}}{J_p + M_a l_n^2} & \dfrac{K_{py}}{J_p + M_a l_n^2} \\ \dfrac{K_{yp}}{J_y + M_a l_n^2\cos^2(x_{11})} & \dfrac{K_{yy}}{J_y + M_a l_n^2\cos^2(x_{11})} \end{bmatrix}. \qquad (7)$$

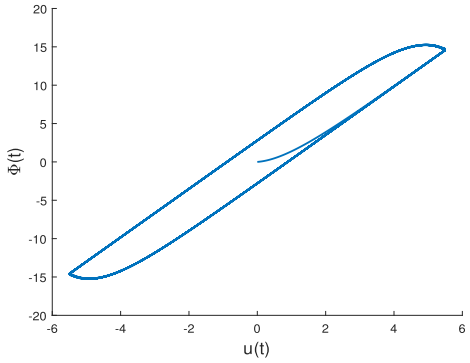

Fig. 2. Hysteresis curve.

Property [55]: The hysteresis-type nonlinearity is defined as

$$\frac{d\Phi(u)}{dt} = k_l\left|\frac{du}{dt}\right|[p_d u - \Phi(u)] + k_v\frac{du}{dt} \qquad (8)$$

where k_l, p_d, and k_v are constants, which satisfy $p_d > 0$ and $p_d > k_v$. According to [55], (8) can be expressed as

$$\Phi_i(u_i) = p_{di}u_i + h_i(u_i), \quad i = 1, 2 \qquad (9)$$

$$\begin{aligned}h_i(u_i) &= (\Phi_{0i} - p_{di}u_{0i})e^{-k_{li}(u_i - u_{0i})\mathrm{sgn}(\dot{u}_i)} \\ &\quad + e^{-k_{li}u_i\mathrm{sgn}(\dot{u}_i)}\int_{u_{0i}}^{u_i}(k_{vi} - p_{di})e^{k_{li}\zeta_j\mathrm{sgn}(\dot{u}_i)}\,d\zeta_j \qquad (10)\end{aligned}$$

where Φ_{0i} and u_{0i} are the initial values of Φ_i and u_i, respectively. This shows that (8) can be used to represent the backlash-like hysteresis shown in Fig. 2, where $k_l = 1$, $p_d = 3.1635$, $k_v = 0.345$, and $u(t) = 5.5\sin(2.3t)$. According to [55], $h_i(u_i)$ is bounded, $|h_i(u_i)| \le h_i^*$ with $h_i^* > 0$, $i = 1, 2, \ldots, n$. The backlash-like hysteresis nonlinearity $\Phi(u)$ can also be expressed as

$$\Phi(u) = P_d u + H(u) \qquad (11)$$

where $P_d = \mathrm{diag}[p_{d1}, p_{d2}]$ with $P_d > 0$ and $H(u) = [h_1(u_1), h_2(u_2)]^T$. $H(u)$ is bounded, i.e., $\|H(u)\| \le H^*$ and $H^* = (h_1^{*2} + h_2^{*2})^{1/2}$.

Assumption 1 [55]: The slope of the backlash-like hysteresis P_d is unknown, and there exists an unknown constant c such that $p_{d1} = p_{d2} = c$.

Remark 1: Since P_d is the slope of backlash-like hysteresis and, in practical situations, the slope of backlash-like hysteresis is often unknown and upper bounded, to solve the backlash-like hysteresis problem in helicopter systems, we consider the case that the slope of hysteresis has the upper bounded maximum value c. In this way, we have $P_d = \mathrm{diag}[p_{d1}, p_{d2}] = c\,\mathrm{diag}[I]_{2\times 2}$.

Substituting (11) into (4) and then from Remark 1, we derive

$$\begin{aligned}\dot{x}_2 &= F(x) + \Delta F(x) + (G(x) + \Delta G(x))(cu + H(u)) \\ &= F(x) + \Delta F(x) + cG(x)u + G(x)H(u) \\ &\quad + \Delta G(x)(cu + H(u)). \qquad (12)\end{aligned}$$

In order to avoid the situation that the inverse matrix of the control gain coefficient $G(x)$ may not exist in the system, we propose $u = G^T(x)\nu$, where ν is an ideal control input

signal. Therefore, (12) can be rewritten as

$$\begin{aligned}\dot{x}_2 &= F(x) + \Delta F(x) + cG(x)G^T(x)\nu + G(x)H(u) \\ &\quad + \Delta G(x)(cu + H(u)) \\ &= F(x) + c\big(G(x)G^T(x) + \gamma\, I_{2\times 2}\big)\nu - \gamma\, I_{2\times 2}\nu \\ &\quad + \Delta F(x) + \Delta G(x)(cu + H(u)) + G(x)H(u) \\ &= F(x) + c\big(G(x)G^T(x) + \gamma\, I_{2\times 2}\big)\nu + P(x,u) + D(x,u)\end{aligned} \tag{13}$$

where $P(x,u) = -\gamma\, I_{2\times 2}\nu + \Delta F(x) + \Delta G(x)(cu + H(u))$ and $\varpi(x,u) = G(x)H(u)$.

B. Preliminaries

Assumption 2: There exists an unknown positive constant G^* satisfying $\|G\| \le G^*$.

Lemma 1 [56]: For Lyapunov function $V(t)$, if the initial value $V(0)$ is bounded, then $V(t)$ is positive definite and continuous. The following inequality is presented:

$$\dot{V}(t) \le -\varsigma V(t) + C_1 \tag{14}$$

where $\varsigma > 0$ and $C_1 > 0$.

Lemma 2 [57]: For the interval $|z(t)| \le q$, $\forall t \in [0, +\infty)$ with q being any positive constant, the following inequality holds:

$$\log \frac{q^2}{q^2 - z^2} \le \frac{z^2}{q^2 - z^2}. \tag{15}$$

Lemma 3 [58]: For any $\mu \in R$ and $\iota > 0$, the inequality $0 \le |\mu| - \mu \tanh(\mu/\iota) \le 0.2785\iota$ holds.

C. Neural Networks

Since the radial basis function NN (RBFNN) has the advantages of local approximation, fast learning speed, and avoiding local minimum problem, we use the following the RBFNN to estimate the unknown nonlinear function in 2-DOF helicopter systems. For nonlinear functions $f(X)$, $R^m \to R$, we have

$$f(X) = W^T O(X) \tag{16}$$

where $X \in \Omega_a \subset R^m$ is the RBFNN input vector, Ω_a is a compact set, $W = [W_1, W_2, \ldots, W_q]^T \in R^q$ is the unknown ideal weight vector, $q > 1$ denotes the node number in the hidden layer, and $O(X) = [O_1(X), O_2(X), \ldots, O_q(X)]^T$. $O_j(X)$ is a neuron activation function that is composed of RBF [59]

$$O_j(X) = \exp\left(\frac{-\big(X - c_j\big)^T\big(X - c_j\big)}{{b_j}^2}\right), \quad j = 1, 2, \ldots, q \tag{17}$$

where $c_j = [c_{j1}, c_{j2}, \ldots, c_{jm}]^T$ is the center vector of the jth hidden layer neuron and b_j is the width vector of Gaussian function. In addition, the RBFNN can approximate a continuous function on a tight set to an arbitrary accuracy as follows:

$$f(X) = W^{*\mathrm{T}} O(X) + \rho(X), \quad \|\rho\| \le \rho^* \tag{18}$$

where $W^{*\mathrm{T}}$ is an ideal weight vector, $\rho(X)$ is the error approximation term, and ρ^* is a positive constant. W^* is defined as

$$W^* = \arg\min_{W \in R^q} \left\{ \sup_{X \in \Omega_a} \left|\left| f(x) - W^T H(X) \right|\right| \right\}. \tag{19}$$

III. Control Design

Considering $|h_i(u_i)| \le h_i^*$ with $h_i^* > 0$ and then according to Assumption 2, we can conclude that $\|\varpi\| \le \varpi^*$ with ϖ^* being an unknown constant.

Define an error variable as

$$z_1 = x_1 - x_d \tag{20}$$

where $x_d = [\theta_d, \phi_d] \in R^2$ is an desired trajectory. The derivative of the position error yields

$$\dot{z}_1 = \dot{x}_1 - \dot{x}_d. \tag{21}$$

Then, define the second error variable as

$$z_2 = x_2 - \alpha \tag{22}$$

with α being the virtual controller of the system.

The time derivative of z_2 is given as

$$\dot{z}_2 = \dot{x}_2 - \dot{\alpha}. \tag{23}$$

Consider the following BLF:

$$V_{\mathrm{BLF}} = \frac{1}{2}\sum_{i=1}^{2} \log \frac{q_i^2}{q_i^2 - z_{1i}^2}. \tag{24}$$

Based on (21), the time derivative of V_1 gives

$$\begin{aligned}\dot{V}_{\mathrm{BLF}} &= \sum_{i=1}^{2} \frac{z_{1i}\dot{z}_{1i}}{q_i^2 - z_{1i}^2} \\ &= \sum_{i=1}^{2} \frac{z_{1i}(x_{2i} - \dot{x}_{di})}{q_i^2 - z_{1i}^2} \\ &= \sum_{i=1}^{2} \frac{z_{1i}(z_{2i} + \alpha_i - \dot{x}_{di})}{q_i^2 - z_{1i}^2}.\end{aligned} \tag{25}$$

A virtual controller is designed as follows:

$$\alpha_i = -k_i z_{1i} + \dot{x}_{di}, \quad i = 1, 2 \tag{26}$$

where $k_i, i = 1, 2$, are the design parameters.

Substitution of (26) into (25) yields

$$\dot{V}_{\mathrm{BLF}} = \sum_{i=1}^{2} \frac{z_{1i}z_{2i} - k_i z_{1i}^2}{q_i^2 - z_{1i}^2}. \tag{27}$$

Consider the following Lyapunov function candidate as

$$V_1 = V_{\mathrm{BLF}} + \frac{1}{2} z_2^T z_2. \tag{28}$$

The time derivative of V_1 leads to

$$\dot{V}_1 = \dot{V}_{\mathrm{BLF}} + z_2^T \dot{z}_2. \tag{29}$$

By substituting (13), (23), and (27) into (29), we have

$$\begin{aligned}\dot{V}_1 &= \dot{V}_{\mathrm{BLF}} + z_2^T(\dot{x}_2 - \dot{\alpha}) \\ &= \sum_{i=1}^{2} \frac{z_{1i}z_{2i} - k_i z_{1i}^2}{q_i^2 - z_{1i}^2} + z_2^T\big(F(x) + c\big(G(x)G^T + \gamma\, I_{2\times 2}\big)\nu \\ &\qquad + P(x,u) + \varpi - \dot{\alpha}\big). \end{aligned} \tag{30}$$

Define $\omega = (1/c)$ with ω being an unknown constant. Since the function $P(x,u)$ is unknown and uncertain, we can use RBFNN to estimate it. Thus, we obtain

$$P(x,u) = W^{*T} O(X) + \rho(X) \tag{31}$$

where W^* is an ideal weight, $O(X)$ contains the activation function, $X = [x_1, x_2, x_d, \dot{x}_d]$ is the input of the NNs, and $\rho(X)$ is an approximation error satisfying $\|\rho(X)\| \le \rho^*$ with $\rho^* > 0$ being an unknown constant. Moreover, the estimated weight is defined as $\hat{W}$ with the weight error $\tilde{W} = \hat{W} - W^*$. We propose the controller as

$$\nu = \hat{\omega}\big(G(x)G^T(x) + \gamma\, I_{2\times 2}\big)^{-1}\psi \tag{32}$$

$$\begin{aligned}\psi = &-F(x) - K_2 z_2 - \begin{bmatrix} \dfrac{z_{11}}{q_1^2 - z_{11}^2} \\ \dfrac{z_{12}}{q_2^2 - z_{12}^2} \end{bmatrix} - \hat{W}^T O(X) \\ &- \tanh\left(\frac{z_2}{b_1}\right)\hat{\varpi}^* + \dot{\alpha}. \end{aligned} \tag{33}$$

According to the backlash-like hysteresis, $\Phi(u) = P_d u + H(u)$ in Property 1, where $H(u)$ is an approximation error. In order to eliminate the effect of hysteresis error and enhance the control accuracy of the system, we construct an adaptive variable $\hat{\varpi}^*$ to compensate for the approximation error $H(u)$.

We define $\tilde{\varpi}^* = \varpi^* - \hat{\varpi}^*$ and $\tilde{\omega} = \omega - \hat{\omega}$. Then, the updating laws of $\dot{\hat{W}}$, $\dot{\hat{\varpi}}^*$, and $\dot{\hat{\omega}}$ are designed as

$$\dot{\hat{W}} = \Gamma_w\big(O(X)z_2^T - \eta_w \hat{W}\big) \tag{34}$$

$$\dot{\hat{\varpi}}^* = \Gamma_\varpi\left(z_2^T \tanh\left(\frac{z_2}{b_1}\right) - \eta_\varpi \hat{\varpi}^*\right) \tag{35}$$

$$\dot{\hat{\omega}} = -\Gamma_\omega\big(z_2^T\psi + \eta_\omega\hat{\omega}\big) \tag{36}$$

where $\Gamma_w = \Gamma_w^T \in R^{n\times n}$, $\Gamma_\varpi > 0$, and $\Gamma_\omega > 0$. Also, η_w, η_ϖ, and η_ω are small positive constants.

Substituting (31)–(33) into (30), we have

$$\begin{aligned}\dot{V}_1 = &\sum_{i=1}^{2} \frac{z_{1i}z_{2i} - k_i z_{1i}^2}{q_i^2 - z_{1i}^2} + z_2^T\left(F(x) + c\left(\frac{1}{c} - \tilde{\omega}\right)\psi + W^{*T}O(X)\right. \\ &\left. + \rho + \varpi - \dot{\alpha}\right) - c\tilde{\omega}\psi \\ = &\sum_{i=1}^{2} \frac{z_{1i}z_{2i} - k_i z_{1i}^2}{q_i^2 - z_{1i}^2} - z_2^T\tilde{W}^T O(X) + z_2^T\rho + z_2^T\varpi \\ &- z_2^T\tanh\left(\frac{z_2}{b_1}\right)\hat{\varpi} - z_2^T K_2 z_2 - z_2^T\begin{bmatrix} \dfrac{z_{11}}{q_1^2 - z_{11}^2} \\ \dfrac{z_{12}}{q_2^2 - z_{12}^2} \end{bmatrix} - cz_2^T\tilde{\omega}\psi \\ = &-\sum_{i=1}^{2} \frac{k_i z_{1i}^2}{q_i^2 - z_{1i}^2} - z_2^T\tilde{W}^T O(X) + z_2^T\rho + z_2^T\varpi \\ &- z_2^T\tanh\left(\frac{z_2}{b_1}\right)\hat{\varpi}^* - z_2^T K_2 z_2 - cz_2^T\tilde{\omega}\psi. \end{aligned} \tag{37}$$

Consider the following inequalities:

$$z_2^T\varpi \le \varpi^* \sum_{i=1}^{2} |z_{2i}| \tag{38}$$

$$z_2^T \tanh\left(\frac{z_2}{b_1}\right) = \sum_{i=1}^{2}\left(z_{2i}\tanh\left(\frac{z_{2i}}{b_1}\right)\right). \tag{39}$$

Invoking Lemma 2, we obtain

$$\sum_{i=1}^{2}|z_{2i}| - \sum_{i=1}^{2}\left(z_{2i}\tanh\left(\frac{z_{2i}}{b_1}\right)\right) \le 0.557 b_1. \tag{40}$$

We then consider the Lyapunov candidate equation as

$$V_2 = V_1 + \mathrm{tr}\left\{\frac{1}{2}\tilde{W}^T\Gamma_w^{-1}\tilde{W}\right\} + \frac{1}{2\Gamma_\varpi}\tilde{\varpi}^{*2} + \frac{c}{2\Gamma_\omega}\tilde{\omega}^2 \tag{41}$$

where $\mathrm{tr}\{\cdot\}$ denotes a trace operation of a matrix. From (41), we known that V_2 is a function of the variables z_1, z_2, W, ϖ^*, and ω.

Substituting (34)–(36) into $\dot{V}_2$ leads to

$$\begin{aligned}\dot{V}_2 = &\dot{V}_1 + \mathrm{tr}\big\{\tilde{W}^T O(X)z_2^T\big\} - \eta_w\mathrm{tr}\big\{\tilde{W}^T\hat{W}\big\} \\ &- z_2^T\tanh\left(\frac{z_2}{b_1}\right)\tilde{\varpi}^* + \eta_\varpi\tilde{\varpi}^*\hat{\varpi}^* + c\tilde{\omega}z_2^T\psi + \eta_\omega\tilde{\omega}\hat{\omega}. \end{aligned} \tag{42}$$

Substituting (37) and (40) into (42), we have

$$\begin{aligned}\dot{V}_2 \le &-\sum_{i=1}^{2}\frac{k_i z_{1i}^2}{q_i^2 - z_{1i}^2} + z_2^T\rho + 0.557 b_1\varpi^* - z_2^T K_2 z_2 \\ &- \eta_w\mathrm{tr}\big\{\tilde{W}^T\hat{W}\big\} + \eta_\varpi\tilde{\varpi}^*\varpi^* - \eta_\varpi\tilde{\varpi}^{*2} + \eta_\omega\tilde{\omega}\omega - \eta_\omega\tilde{\omega}^2 \end{aligned} \tag{43}$$

where $z_2^T\rho \le (1/2)z_2^T z_2 + (1/2)\rho^{*2}$.

Employing Young's inequality results in

$$-\eta_w\mathrm{tr}\big\{\tilde{W}^T\hat{W}\big\} \le -\frac{\eta_w}{2}\|\tilde{W}\|_F^2 + \frac{\eta_w}{2}\|W^*\|_F^2 \tag{44}$$

$$\eta_\varpi\tilde{\varpi}^*\varpi^* \le \frac{1}{\sigma_1}\eta_\varpi\tilde{\varpi}^{*2} + \sigma_1\eta_\varpi\varpi^{*2} \tag{45}$$

$$\eta_\omega\tilde{\omega}\omega \le \frac{1}{\sigma_2}\eta_\omega\tilde{\omega}^2 + \sigma_2\eta_\omega\omega^2 \tag{46}$$

where $\|\cdot\|$ is the Frobenius norm of a vector or a matrix.

Substituting (44)–(46) into (43), we derive

$$\begin{aligned}\dot{V}_2 \le &-\sum_{i=1}^{2}\frac{k_i z_{1i}^2}{q_i^2 - z_{1i}^2} + \frac{1}{2}z_2^T z_2 + \frac{1}{2}\rho^{*2} - z_2^T K_2 z_2 \\ &- \frac{\eta_w}{2}\|\tilde{W}\|_F^2 + \frac{\eta_w}{2}\|W^*\|_F^2 - \left(1 - \frac{1}{\sigma_1}\right)\eta_\varpi\tilde{\varpi}^{*2} + \sigma_1\eta_\varpi\varpi^{*2} \\ &- \left(1 - \frac{1}{\sigma_2}\right)\eta_\omega\tilde{\omega}^2 + \sigma_2\eta_\omega\omega^2 + 0.557 b_1\varpi^* \end{aligned} \tag{47}$$

where σ_1 and σ_2 are design parameters.

According to Lemmas 1 and 2, we obtain

$$\begin{aligned}\dot{V}_2 \le &-\sum_{i=1}^{2} k_i \log\frac{z_{1i}^2}{q_i^2 - z_{1i}^2} - z_2^T\left(K_2 - \frac{1}{2}I\right)z_2 - \frac{\eta_w}{2}\|\tilde{W}\|_F^2 \\ &- \left(1 - \frac{1}{\sigma_1}\right)\eta_\varpi\tilde{\varpi}^{*2} - \left(1 - \frac{1}{\sigma_2}\right)\eta_\omega\tilde{\omega}^2 + \frac{1}{2}\rho^{*2} \\ &+ \frac{\eta_w}{2}\|W^*\|_F^2 + \sigma_1\eta_\varpi\varpi^{*2} + \sigma_2\eta_\omega\omega^2 + 0.557 d_1\varpi^* \\ \le &\ \varsigma V_2 + \Xi \end{aligned} \tag{48}$$

where

$$\varsigma = \min\left(2\min(k_i), 2\lambda_{\min}\left(K_2 - \frac{1}{2}I\right), \frac{2\eta_w}{\lambda_{\max}\left(\Gamma_w^{-1}\right)}, 2\Gamma_\varpi \eta_\varpi \lambda_{\min}\left(1 - \frac{1}{\sigma_1}\right), 2\Gamma_\omega \eta_\omega \lambda_{\min}\left(1 - \frac{1}{\sigma_2}\right)\right) \tag{49}$$

$$\Xi = \frac{1}{2}\rho^{*2} + \frac{\eta_w}{2}\|W^*\|_F^2 + \sigma_1 \eta_\varpi \varpi^{*2} + \sigma_2 \eta_\omega \omega^2 + 0.557 b_1 \varpi^* \tag{50}$$

with

$$\min(k_i) > 0, \quad \lambda_{\min}\left(K_2 - \frac{1}{2}I\right) > 0$$
$$\left(1 - \frac{1}{\sigma_1}\right) > 0, \quad \left(1 - \frac{1}{\sigma_2}\right) > 0. \tag{51}$$

Theorem: For the 2-DOF helicopter system given by (1) and (2), with the application of the presented NN controllers (32) and (33), and adaptive updating laws (34)–(36), we conclude that z_1, z_2, W, ϖ^*, and ω are semiglobally bounded. In addition, the tracking errors z_1 and z_2 and approximation errors $\tilde{W}$, $\tilde{\varpi}^*$, and $\tilde{\omega}$ converge to their respective compact sets Ω_{z_1}, Ω_{z_2}, $\Omega_{\tilde{W}}$, $\Omega_{\tilde{\varpi}^*}$, and $\Omega_{\tilde{\omega}}$, respectively, defined as

$$\Omega_{z_1} = \left\{z_1 \in R^2 \middle| |z_{1i}| \le \sqrt{q_i^2\left(1 - e^{-\Delta}\right)}\right\} \tag{52}$$

$$\Omega_{z_2} = \left\{z_2 \in R^2 \middle| \|z_2\| \le \sqrt{\Delta}\right\} \tag{53}$$

$$\Omega_{\tilde{W}} = \left\{\tilde{W} \in R^{q\times 2} \middle| \|\tilde{W}\| \le \sqrt{\frac{\Delta}{\lambda_{\min}\left(\Gamma_w^{-1}\right)}}\right\} \tag{54}$$

$$\Omega_{\tilde{\varpi}^*} = \left\{\tilde{\varpi}^* \middle| \left|\tilde{\varpi}^*\right| \le \sqrt{\Gamma_\varpi \Delta}\right\} \tag{55}$$

$$\Omega_{\tilde{\omega}} = \left\{\tilde{\omega} \middle| |\tilde{\omega}| \le \sqrt{\Gamma_\omega \Delta}\right\} \tag{56}$$

where $\Delta = 2(V_2(0) + (\Xi/\varsigma))$, and ς and Ξ are defined in (49) and (50), respectively.

Proof: Multiplying (48) by $e^{\varsigma t}$ yields

$$\frac{\mathrm{d}}{\mathrm{d}t}\left(V_3 e^{\varsigma t}\right) \le \Xi e^{\varsigma t}. \tag{57}$$

Integrating (57), we obtain

$$V_2 \le \left(V_2(0) - \frac{\Xi}{\varsigma}\right)e^{-\varsigma t} + \frac{|z_{1i}|}{\varsigma}. \tag{58}$$

Thus, for z_1, we obtain

$$\frac{1}{2}\log\frac{q_i^2}{q_i^2 - z_{1i}^2} \le V_3(0) + \frac{|z_{1i}|}{\varsigma}$$
$$|z_{1i}| \le \sqrt{q_i^2\left(1 - e^{-\Delta}\right)}. \tag{59}$$

Similarly, for z_2, $\tilde{W}$, $\tilde{\varpi}^*$, and $\tilde{\omega}$, we further have

$$\|z_2\| \le \sqrt{\Delta} \tag{60}$$

$$\|\tilde{W}\| \le \sqrt{\frac{\Delta}{\lambda_{\min}\left(\Gamma_w^{-1}\right)}} \tag{61}$$

$$|\tilde{\varpi}^*| \le \sqrt{\Gamma_\varpi \Delta} \tag{62}$$

$$|\tilde{\omega}| \le \sqrt{\Gamma_\omega \Delta}. \tag{63}$$

TABLE I
SYSTEM PARAMETERS

symbol	Value	Unit	symbol	Value	Unit
J_p	0.0215	kg·m^2	l_n	0.0071	m
J_y	0.0237	kg·m^2	K_{pp}	0.0011	N·m/V
M_a	1.0750	kg	K_{py}	0.0021	N·m/V
D_p	0.0071	N/V	K_{yp}	-0.0027	N·m/V
D_y	0.0220	N/V	K_{yy}	0.0022	N·m/V

Remark 2: In this study, for the backlash-like hysteresis $\Phi(u) = P_d u + H(u)$, $H(u)$ is an approximation error. The adaptive NN controller proposed uses an adaptive variable $\hat{\varpi}^*$ to compensate for $H(u)$. The effect of backlash-like hysteresis can be reduced, thus improving the control accuracy of the system.

Remark 3: In [27] and [28], an NN output feedback control was employed to stabilize the UAV system with the position and attitude measurement. Different from [27] and [28], this study aims to address the hysteresis and output constraint in the 2-DOF helicopter system. The adaptive variable $\hat{\varpi}^*$ is used to deal with the hysteresis and the BLF is employed to resolve the output constraint presented in the system.

IV. NUMERICAL SIMULATION

In this section, the presented algorithms are verified through simulation examples of a Quanser's 2-DOF helicopter system. Table I shows the parameters of the Quanser's laboratory platform used in the simulation.

The initial values of the angles are chosen as $x_1 = [0, 0]^{\mathrm{T}}$, and then, the desired tracking trajectory is set as $x_d = [(5\pi/36)\sin(t), (\pi/18)\sin(t)]^{\mathrm{T}}$.

The initial values of the weights in the NN are zero. The detailed control parameters are designed as $k_1 = 50$, $k_2 = 50$, $K_2 = \mathrm{diag}[60, 60]$, $\gamma = 1$, $\Gamma_w = 64 I_{64\times 64}$, $\Gamma_\varpi = 15$, $\Gamma_\omega = 15$, $\eta_w = 0.2$, $\eta_\varpi = 0.1$, and $\eta_\omega = 0.1$. The parameters of the hysteresis-type nonlinearity are designed as $k_l = 1$, $p_d = 3.1635$, and $k_v = 2$. The bound of the tracking error is selected as $q = [0.09, 0.03]^T$.

A. Case 1: Under the Proposed Control Scheme

The numerical simulation results are shown in Fig. 3(a) and (d). It can be seen from Fig. 3(a) and (b) that x_{11} and x_{12} can fully track their desired trajectories. Fig. 3(c) shows the tracking errors of the system. Fig. 3(d) represents the control input of the system. In addition, it is evident from Fig. 3(a) and (b) that the controller design does not violate the output constraints. From Fig. 3(c), we find that the error of the system converges to a very small range near zero and the stability of the system is better. Therefore, the control algorithm designed in this study is effective for trajectory tracking control of a helicopter system with backlash-like hysteresis and output constraints.

B. Case 2: Under the Proposed Control Scheme Without Backlash-Like Hysteresis Compensation

This case demonstrates the simulation results without backlash-like hysteresis compensation in the algorithm proposed in this article. The design parameters required in this

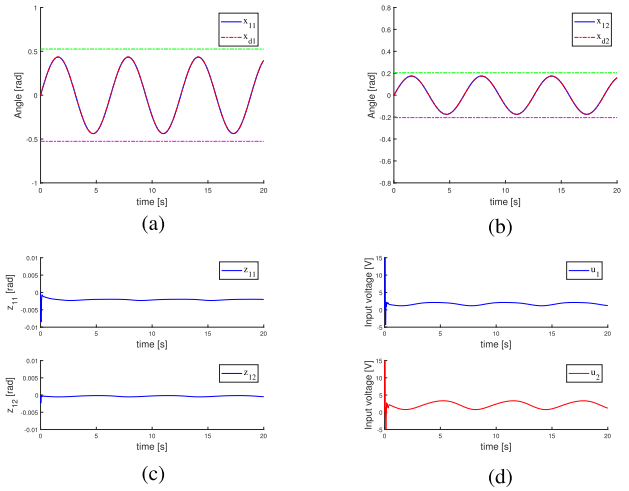

Fig. 3. Under the proposed control scheme. (a) Tracking performance of x_{11}. (b) Tracking performance of x_{12}. (c) Tracking errors: z_{11} and z_{12}. (d) Control input u.

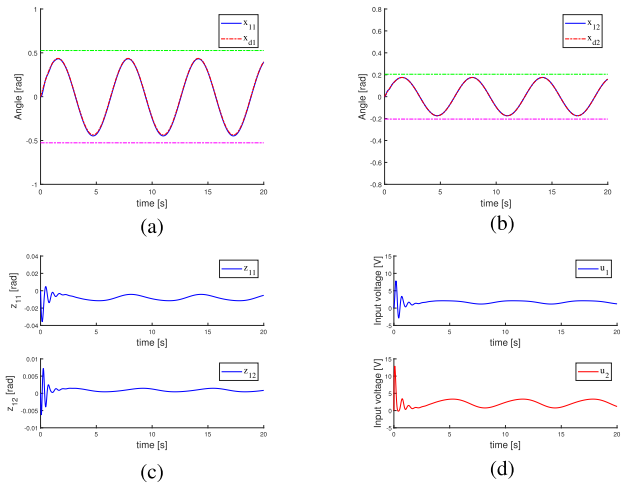

Fig. 4. Under the proposed control scheme without backlash-like hysteresis compensation. (a) Tracking performance of x_{11}. (b) Tracking performance of x_{12}. (c) Tracking errors: z_{11} and z_{12}. (d) Control input u.

case are the same as in Case 1. Fig. 4(a) and (b) shows the tracking response of the system between the output variables and the desired trajectory, and in addition, it can be seen that the output variables do not violate the output constraint. Fig. 4(c) shows the tracking error response of the system. Fig. 4(d) represents the control inputs of the system.

Compared with Case 1, the output variables in Case 2 do not track the desired trajectory and the tracking error is larger. In addition, the control input of the system oscillates at the beginning of the period, making the input of the system unstable.

V. Experimental Results

To further verify the effectiveness of the proposed controller, we conducted experiments on a Quanser's 2-DOF helicopter platform in Fig. 5. Moreover, in practice, the input range of the two voltages of the 2-DOF helicopter is $[-24, \ +24\ \text{V}]$.

A. Case 1: Under the Proposed Control Scheme

In this case, we validate the control algorithm proposed in this article. Fig. 6(a) and (b) shows the tracking effects of

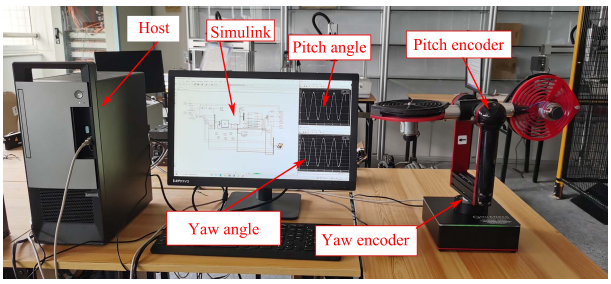

Fig. 5. Experiment setup.

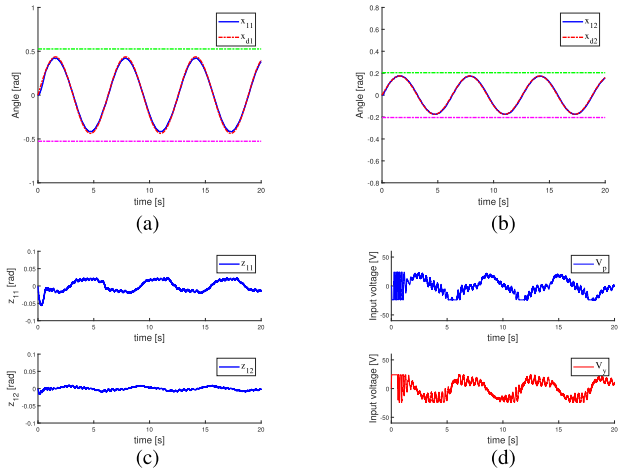

Fig. 6. Under the proposed control scheme. (a) Tracking performance of x_{11}. (b) Tracking performance of x_{12}. (c) Tracking errors: z_{11} and z_{12}. (d) Control input u.

the output variables of the system with respect to the desired trajectories. Fig. 6(c) shows the tracking error response of the system. Fig. 6(d) shows the motor voltage input of the helicopter system. The experimental results show that under the action of this controller, the output variables of the system can meet the tracking requirements with a smaller tracking error, and the input of the system also has a good trajectory response, which proves the effectiveness and rationality of the control strategy proposed in this study.

B. Case 2: Under the Proposed Control Scheme Without Backlash-Like Hysteresis Compensation

In this case, the backlash-like hysteresis compensation is not considered in the control strategy proposed in this study, and the experimental results obtained are shown in Fig. 7(a) and (d). Fig. 7(a) and (b) shows the performance of x_{11} and x_{12} of the desired trajectory tracking, and Fig. 7(c) shows the tracking error of the system. Fig. 7(d) shows the control input of the system.

As can be seen in Fig. 7(a) and (b), the system output variables do not violate the output constraints under this control strategy. Meanwhile, we observe from Fig. 8 that the fluctuation of the error in this case is larger compared with Case 1, and the system tracking effect is not satisfactory. This also shows that without hysteresis compensation, the NN alone does not eliminate the effects caused by backlash-like hysteresis.

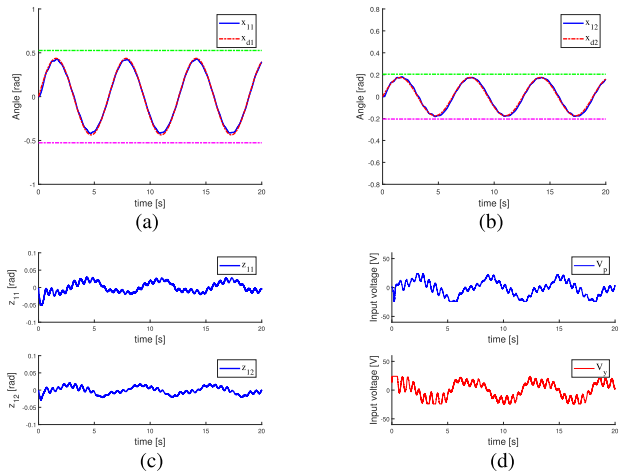

Fig. 7. Under the proposed control scheme without backlash-like hysteresis compensation. (a) Tracking performance of x_{11}. (b) Tracking performance of x_{12}. (c) Tracking errors: z_{11} and z_{12}. (d) Control input u.

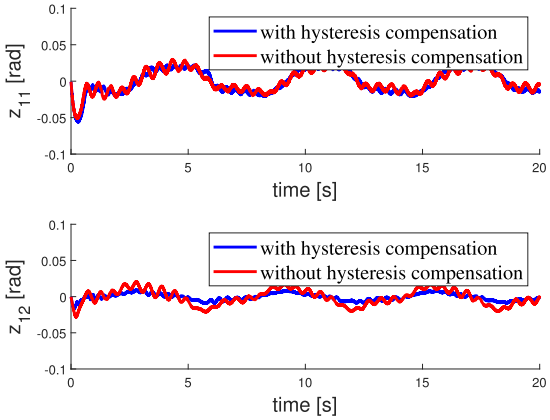

Fig. 8. Tracking error with and without backlash-like hysteresis compensation.

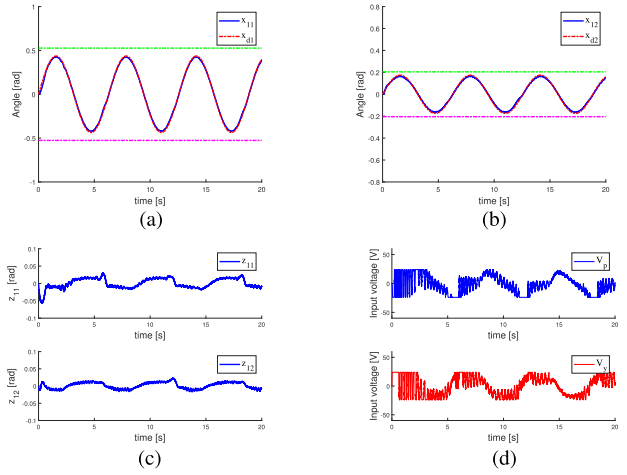

Fig. 9. With adaptive control. (a) Tracking performance of x_{11} with adaptive control. (b) Tracking performance of x_{12}. (c) Tracking errors: z_{11} and z_{12}. (d) Control input u.

C. Case 3: Adaptive Control

To demonstrate the superiority of NN control, an adaptive control scheme is compared in this case. Fig. 9(a) and (b) shows the ability of the system's variables to follow the desired trajectory. Fig. 9(c) shows the variation of the tracking error of the system. Fig. 9(d) shows the control input of the system.

Compared with Case 1, the tracking error, in this case, is larger, indicating that the performance of system output variables in tracking the desired trajectory is less than an ideal case, and at the same time, the control input trajectory of the system is more volatile. From the above results, it can be shown that the robustness of the system is poor under the adaptive control.

VI. Conclusion

An adaptive NN control was proposed for the uncertain 2-DOF helicopter system with unknown backlash-like hysteresis and output constraints. The RBFNN was used to estimate the uncertainty of the system, and then, the adaptive variables were developed to address the effects of backlash-like hysteresis present in the system. With the BLF technology to deal with the output constraint of the system, the Lyapunov method proved that the system was uniformly bounded. Finally, simulations and experiments validated the effectiveness and validity of the proposed control strategy.

References

[1] F. Chen, Q. Wu, B. Jiang, and G. Tao, "A reconfiguration scheme for quadrotor helicopter via simple adaptive control and quantum logic," *IEEE Trans. Ind. Electron.*, vol. 62, no. 7, pp. 4328–4335, Jul. 2015.

[2] Z. Liu, Z. Han, Z. Zhao, and W. He, "Modeling and adaptive control for a spatial flexible spacecraft with unknown actuator failures," *Sci. China Inf. Sci.*, vol. 64, no. 5, pp. 1–16, May 2021.

[3] W. He, X. Mu, L. Zhang, and Y. Zou, "Modeling and trajectory tracking control for flapping-wing micro aerial vehicles," *IEEE/CAA J. Automatica Sinica*, vol. 8, no. 1, pp. 148–156, Jan. 2021.

[4] W. He, T. Wang, X. He, L. Yang, and O. Kaynak, "Dynamical modeling and boundary vibration control of a rigid-flexible wing system," *IEEE/ASME Trans. Mechatronics*, vol. 25, no. 6, pp. 2711–2721, Dec. 2020.

[5] B. Luo, H. N. Wu, and T. Huang, "Optimal output regulation for model-free quanser helicopter with multistep Q-learning," *IEEE Trans. Ind. Electron.*, vol. 65, no. 6, pp. 4953–4961, Jun. 2018.

[6] S.-K. Kim and C. K. Ahn, "Performance-boosting attitude control for 2-DOF helicopter applications via surface stabilization approach," *IEEE Trans. Ind. Electron.*, vol. 69, no. 7, pp. 7234–7243, Jul. 2022.

[7] M. Hernandez-Gonzalez, A. Y. Alanis, and E. A. Hernandez-Vargas, "Decentralized discrete-time neural control for a Quanser 2-DOF helicopter," *J. Appl. Soft Comp.*, vol. 12, no. 8, pp. 2462–2469, Aug. 2012.

[8] L. Dutta and D. K. Das, "Adaptive model predictive control design using multiple model second level adaptation for parameter estimation of two-degree freedom of helicopter model," *Int. J. Robust Nonlinear Control*, vol. 31, no. 8, pp. 3248–3278, May 2021.

[9] C.-W. Kuo, C.-C. Tsai, and C.-T. Lee, "Intelligent leader-following consensus formation control using recurrent neural networks for small-size unmanned helicopters," *IEEE Trans. Syst., Man, Cybern. Syst.*, vol. 51, no. 2, pp. 1288–1301, Feb. 2021.

[10] Y. Zhu, B. Zhu, H. H. T. Liu, and K. Qin, "A model-based approach for measurement noise estimation and compensation in feedback control systems," *IEEE Trans. Instrum. Meas.*, vol. 69, no. 10, pp. 8112–8127, Oct. 2020.

[11] S. P. Sadala and B. M. Patre, "Super-twisting control using higher order disturbance observer for control of SISO and MIMO coupled systems," *ISA Trans.*, vol. 106, pp. 303–317, Nov. 2020.

[12] T. Y. Chun, J. B. Park, and Y. H. Choi, "Reinforcement Q-learning based on multirate generalized policy iteration and its application to a 2-DOF helicopter," *Int. J. Control, Autom. Syst.*, vol. 16, no. 1, pp. 377–386, Feb. 2018.

[13] R. G. Subramanian and V. K. Elumalai, "Robust MRAC augmented baseline LQR for tracking control of 2 DoF helicopter," *Robot. Auto. Syst.*, vol. 86, pp. 70–77, Dec. 2016.

[14] E. V. Kumar, G. S. Raaja, and J. Jerome, "Adaptive PSO for optimal LQR tracking control of 2 DoF laboratory helicopter," *Appl. Soft Comput.*, vol. 41, pp. 77–90, Apr. 2016.

[15] I. A. Raptis, K. P. Valavanis, and G. J. Vachtsevanos, "Linear tracking control for small-scale unmanned helicopters," *IEEE Trans. Control Syst. Technol.*, vol. 20, no. 4, pp. 995–1010, Jul. 2012.

[16] I. A. Raptis, K. P. Valavanis, and W. A. Moreno, "A novel nonlinear backstepping controller design for helicopters using the rotation matrix," *IEEE Trans. Control Syst. Technol.*, vol. 19, no. 2, pp. 465–473, Mar. 2011.

[17] H. Rojas-Cubides, J. Cortés-Romero, H. Coral-Enriquez, and H. Rojas-Cubides, "Sliding mode control assisted by GPI observers for tracking tasks of a nonlinear multivariable twin-rotor aerodynamical system," *Control Eng. Pract.*, vol. 88, pp. 1–15, Jul. 2019.

[18] K. Anis and G. Tarek, "An improved robust predictive control approach based on generalized 3rd order S-PARAFAC Volterra model applied to a 2-DoF helicopter system," *Int. J. Control, Autom. Syst.*, vol. 19, no. 4, pp. 1618–1632, Apr. 2021.

[19] Y. Song and J. Guo, "Neuro-adaptive fault-tolerant tracking control of Lagrange systems pursuing targets with unknown trajectory," *IEEE Trans. Ind. Electron.*, vol. 64, no. 5, pp. 3913–3920, May 2017.

[20] R. Moghadam, P. Natarajan, and S. Jagannathan, "Online optimal adaptive control of partially uncertain nonlinear discrete-time systems using multilayer neural networks," *IEEE Trans. Neural Netw. Learn. Syst.*, early access, Mar. 12, 2021, doi: 10.1109/TNNLS.2021.3061414.

[21] H. Gao, Y. Song, and C. Wen, "Event-triggered adaptive neural network controller for uncertain nonlinear system," *Inf. Sci.*, vol. 506, pp. 148–160, Jan. 2020.

[22] C. Sun, W. He, and J. Hong, "Neural network control of a flexible robotic manipulator using the lumped spring-mass model," *IEEE Trans. Syst., Man, Cybern., Syst.*, vol. 47, no. 8, pp. 1863–1874, Aug. 2017.

[23] M. Chen, P. Shi, and C. Lim, "Adaptive neural fault-tolerant control of a 3-DOF model helicopter system," *IEEE Trans. Syst., Man, Cybern. Syst.*, vol. 46, no. 2, pp. 260–270, Feb. 2016.

[24] X. Yang and X. Zheng, "Adaptive NN backstepping control design for a 3-DOF helicopter: Theory and experiments," *IEEE Trans. Ind. Electron.*, vol. 67, no. 5, pp. 3967–3979, May 2020.

[25] S. Shen and J. Xu, "Adaptive neural network-based active disturbance rejection flight control of an unmanned helicopter," *Aerosp. Sci. Technol.*, vol. 119, Dec. 2021, Art. no. 107062.

[26] N. P. Nguyen, N. X. Mung, L. N. N. Thanh Ha, T. T. Huynh, and S. K. Hong, "Finite-time attitude fault tolerant control of quadcopter system via neural networks," *Mathematics*, vol. 8, no. 9, p. 1541, Sep. 2020.

[27] T. Dierks and S. Jagannathan, "Output feedback control of a quadrotor UAV using neural networks," *IEEE Trans. Neural Netw.*, vol. 21, no. 1, pp. 50–66, Jan. 2010.

[28] D. Nodland, H. Zargarzadeh, and S. Jagannathan, "Neural network-based optimal adaptive output feedback control of a helicopter UAV," *IEEE Trans. Neural Netw.*, vol. 24, no. 7, pp. 1061–1073, Jul. 2013.

[29] X. Huo, L. Ma, X. Zhao, B. Niu, and G. Zong, "Observer-based adaptive fuzzy tracking control of MIMO switched nonlinear systems preceded by unknown backlash-like hysteresis," *Inf. Sci.*, vol. 409, pp. 369–386, Jul. 2019.

[30] Z. Liu, G. Lai, Y. Zhang, X. Chen, and C. L. P. Chen, "Adaptive neural control for a class of nonlinear time-varying delay systems with unknown hysteresis," *IEEE Trans. Neural Netw. Learn. Syst.*, vol. 25, no. 12, pp. 2129–2140, Dec. 2014.

[31] Y.-J. Liu, S. Tong, C. L. P. Chen, and D.-J. Li, "Neural controller design-based adaptive control for nonlinear MIMO systems with unknown hysteresis inputs," *IEEE Trans. Cybern.*, vol. 46, no. 1, pp. 9–19, Jan. 2016.

[32] Z. Yu, S. Li, Z. Yu, and F. Li, "Adaptive neural output feedback control for nonstrict-feedback stochastic nonlinear systems with unknown backlash-like hysteresis and unknown control directions," *IEEE Trans. Neural Netw. Learn. Syst.*, vol. 29, no. 4, pp. 1147–1160, Apr. 2018.

[33] L. Liu and L. Tang, "Partial state constraints-based control for nonlinear systems with backlash-like hysteresis," *IEEE Trans. Syst., Man, Cybern., Syst.*, vol. 50, no. 8, pp. 3100–3104, Jun. 2020.

[34] Z. Zhu, Y. Pan, Q. Zhou, and C. Lu, "Event-triggered adaptive fuzzy control for stochastic nonlinear systems with unmeasured states and unknown backlash-like hysteresis," *IEEE Trans. Fuzzy Syst.*, vol. 29, no. 5, pp. 1273–1283, May 2021.

[35] H. Wang, B. Chen, K. Liu, X. Liu, and C. Lin, "Adaptive neural tracking control for a class of nonstrict-feedback stochastic nonlinear systems with unknown backlash-like hysteresis," *IEEE Trans. Neural Netw. Learn. Syst.*, vol. 25, no. 5, pp. 947–958, May 2014.

[36] L. Liu and L. Tang, "Partial state constraints-based control for nonlinear systems with backlash-like hysteresis," *IEEE Trans. Syst., Man, Cybern., Syst.*, vol. 50, no. 8, pp. 3100–3104, Jun. 2020.

[37] L. Kong, Q. Lai, Y. Ouyang, Q. Li, and S. Zhang, "Neural learning control of a robotic manipulator with finite-time convergence in the presence of unknown backlash-like hysteresis," *IEEE Trans. Syst., Man, Cybern. Syst.*, vol. 52, no. 3, pp. 1916–1927, Mar. 2022.

[38] Z. Zhao, Z. Liu, W. He, K.-S. Hong, and H.-X. Li, "Boundary adaptive fault-tolerant control for a flexible Timoshenko arm with backlash-like hysteresis," *Automatica*, vol. 130, Aug. 2021, Art. no. 109690.

[39] W. He, D. O. Amoateng, C. Yang, and D. Gong, "Adaptive neural network control of a robotic manipulator with unknown backlash-like hysteresis," *IET Control Theory Appl.*, vol. 11, no. 4, pp. 567–575, Feb. 2017.

[40] Z. Guo, H. Xue, and Y. Pan, "Neural networks-based adaptive tracking control of multi-agent systems with output-constrained and unknown hysteresis," *Neurocomputing*, vol. 458, pp. 24–32, Oct. 2021.

[41] R. Rout, R. Cui, and Z. Han, "Modified Line-of-Sight guidance law with adaptive neural network control of underactuated marine vehicles with state and input constraints," *IEEE Trans. Control Syst. Technol.*, vol. 28, no. 5, pp. 1902–1914, Sep. 2020.

[42] Y. Cao, C. Wen, and Y. Song, "Prescribed performance control of strict-feedback systems under actuation saturation and output constraint via event-triggered approach," *Int. J. Robust Nonlinear Control*, vol. 29, no. 18, pp. 6357–6373, Dec. 2019.

[43] B. Fan, Q. M. Yang, S. Jagannathan, and Y. X. Sun, "Output-constrained control of nonaffine multiagent systems with partially unknown control directions," *IEEE Trans. Autom. Control*, vol. 64, no. 9, pp. 3936–3942, Jan. 2019.

[44] Y. Li, B. Niu, G. Zong, J. Zhao, and X. Zhao, "Command filter-based adaptive neural finite-time control for stochastic nonlinear systems with time-varying full-state constraints and asymmetric input saturation," *Int. J. Syst. Sci.*, vol. 53, no. 1, pp. 199–221, Jan. 2022.

[45] L. Chen, R. Cui, C. Yang, and W. Yan, "Adaptive neural network control of underactuated surface vessels with guaranteed transient performance: Theory and experimental results," *IEEE Trans. Ind. Electron.*, vol. 67, no. 5, pp. 4024–4035, May 2020.

[46] Y. Li, R. Cui, Z. Li, and D. Xu, "Neural network approximation based near-optimal motion planning with kinodynamic constraints using RRT," *IEEE Trans. Ind. Electron.*, vol. 65, no. 11, pp. 8718–8729, Nov. 2018.

[47] X. Huo, H. R. Karimi, X. Zhao, B. Wang, and G. Zong, "Adaptive-critic design for decentralized event-triggered control of constrained nonlinear interconnected systems within an identifier-critic framework," *IEEE Trans. Cybern.*, early access, Jan. 5, 2021, doi: 10.1109/TCYB.2020.3037321.

[48] K. Zhao, Y. Song, and Z. Zhang, "Tracking control of MIMO nonlinear systems under full state constraints: A single-parameter adaptation approach free from feasibility conditions," *Automatica*, vol. 107, pp. 52–60, Sep. 2019.

[49] Z. Zhao, W. He, and S. S. Ge, "Adaptive neural network control of a fully actuated marine surface vessel with multiple output constraints," *IEEE Trans. Control Syst. Technol.*, vol. 22, no. 4, pp. 1536–1543, Jul. 2016.

[50] K. P. Tee, S. S. Ge, and E. H. Tay, "Barrier Lyapunov functions for the control of output-constrained nonlinear systems," *Automatica*, vol. 45, no. 4, pp. 918–927, Apr. 2009.

[51] K. Zhao and Y. Song, "Removing the feasibility conditions imposed on tracking control designs for state-constrained strict-feedback systems," *IEEE Trans. Autom. Control*, vol. 64, no. 3, pp. 1265–1272, Mar. 2019.

[52] K. Zhao and J. Chen, "Adaptive neural quantized control of MIMO nonlinear systems under actuation faults and time-varying output constraints," *IEEE Trans. Neural Netw. Learn. Syst.*, vol. 31, no. 9, pp. 3471–3481, Sep. 2020.

[53] K. Zhao, Y. Song, W. Meng, C. L. P. Chen, and L. Chen, "Low-cost approximation-based adaptive tracking control of output-constrained nonlinear systems," *IEEE Trans. Neural Netw. Learn. Syst.*, vol. 32, no. 11, pp. 4890–4900, Nov. 2021.

[54] *Quanser AERO Laboratory Guide*, Quanser Inc., Markham, ON, Canada, 2016.

[55] C.-Y. Su, Y. Stepanenko, J. Svoboda, and T. P. Leung, "Robust adaptive control of a class of nonlinear systems with unknown backlash-like hysteresis," *IEEE Trans. Autom. Control*, vol. 45, no. 12, pp. 2427–2432, Dec. 2000.

[56] K. P. Tee and S. S. Ge, "Control of nonlinear systems with partial state constraints using a barrier Lyapunov function," *Int. J. Control*, vol. 84, no. 12, pp. 2008–2023, 2011.

[57] B. Ren, S. S. Ge, K. P. Tee, and T. H. Lee, "Adaptive neural control for output feedback nonlinear systems using a barrier Lyapunov function," *IEEE Trans. Neural Netw.*, vol. 21, no. 8, pp. 1339–1345, Aug. 2010.
[58] Z. Yu, S. Li, Z. Yu, and F. Li, "Adaptive neural output feedback control for nonstrict-feedback stochastic nonlinear systems with unknown backlash-like hysteresis and unknown control directions," *IEEE Trans. Neural Netw. Learn. Syst.*, vol. 29, no. 4, pp. 1147–1160, Apr. 2018.
[59] Z. Zhao, Y. Ren, C. Mu, T. Zou, and K.-S. Hong, "Adaptive neural-network-based fault-tolerant control for a flexible string with composite disturbance observer and input constraints," *IEEE Trans. Cybern.*, early access, Jul. 7, 2021, doi: 10.1109/TCYB.2021.3090417.

Zhijia Zhao (Member, IEEE) received the B.Eng. degree in automatic control from the North China University of Water Resources and Electric Power, Zhengzhou, China, in 2010, and the M.Eng. and Ph.D. degrees in automatic control from the South China University of Technology, Guangzhou, China, in 2013 and 2017, respectively.

He is currently an Associate Professor with the School of Mechanical and Electrical Engineering, Guangzhou University, Guangzhou. His research interests include adaptive and learning control, flexible mechanical systems, and robotics.

Jian Zhang received the B.Eng. degree from West Anhui University, Luan, China, in 2020. He is currently pursuing the master's degree with the School of Mechanical and Electrical Engineering, Guangzhou University, Guangzhou, China.

His research interests include adaptive control, intelligent control, and robotics.

Zhijie Liu (Member, IEEE) received the B.Sc. degree from the China University of Mining and Technology Beijing, Beijing, China, in 2014, and the Ph.D. degree from Beihang University, Beijing, in 2019.

In 2017, he was a Research Assistant with the Department of Electrical Engineering, University of Notre Dame, Notre Dame, IN, USA, for 12 months. He is currently an Associate Professor with the School of Automation and Electrical Engineering, University of Science and Technology Beijing, Beijing. His research interests include adaptive control, modeling and vibration control for flexible structures, and distributed parameter systems.

Chaoxu Mu (Senior Member, IEEE) received the Ph.D. degree in control science and engineering from the School of Automation, Southeast University, Nanjing, China, in 2012.

She was a Visiting Ph.D. Student with the Royal Melbourne Institute of Technology University, Melbourne, VIC, Australia, from 2010 to 2011. She was a Post-Doctoral Fellow with the Department of Electrical, Computer and Biomedical Engineering, The University of Rhode Island, Kingston, RI, USA, from 2014 to 2016. She is currently a Professor with the School of Electrical and Information Engineering, Tianjin University, Tianjin, China. She has authored more than 100 journal articles and conference papers and coauthored two monographs. Her current research interests include nonlinear system control and optimization, and adaptive and learning systems.

Keum-Shik Hong (Fellow, IEEE) received the B.S. degree in mechanical design from Seoul National University, Seoul, South Korea, in 1979, the M.S. degree in mechanical engineering from Columbia University, New York, NY, USA, in 1987, and the M.S. degree in applied mathematics and the Ph.D. degree in mechanical engineering from the University of Illinois at Urbana–Champaign, Champaign, IL, USA, in 1991.

He joined the School of Mechanical Engineering, Pusan National University, Busan, South Korea, in 1993. His research interests include brain–computer interface, nonlinear systems theory, adaptive control, and distributed parameter systems.

Dr. Hong is a fellow of the Korean Academy of Science and Technology, an ICROS Fellow, and a member of the National Academy of Engineering of Korea. He was a recipient of many awards, including the Best Paper Award from the KFSTS of Korea in 1999 and the Presidential Award of Korea in 2007. He was the past President of the Institute of Control, Robotics and Systems (ICROS), South Korea, and is the President of the Asian Control Association. He served as an Associate Editor for *Automatica* from 2000 to 2006 and the Editor-in-Chief for the *Journal of Mechanical Science and Technology* from 2008 to 2011. He is serving as the Editor-in-Chief for the *International Journal of Control, Automation, and Systems*.